




Article

The Potential of Fractional Order Distributed MPC Applied to Steam/Water Loop in Large Scale Ships

Shiquan Zhao ^{1,2,3,*} , Ricardo Cajo ^{1,3,4} , Robain De Keyser ^{1,3} and Clara-Mihaela Ionescu ^{1,3,5} 

¹ Research Group on Dynamical Systems and Control, Department of Electromechanical, Systems and Metal Engineering, Ghent University, B-9052 Ghent, Belgium; RicardoAlfredo.CajoDiaz@UGent.be (R.C.); Robain.DeKeyser@ugent.be (R.D.K.); ClaraMihaela.Ionescu@ugent.be (C.-M.I.)

² College of Automation, Harbin Engineering University, Harbin 150001, China

³ EEDT Decision & Control, Flanders Make, B-9052 Ghent, Belgium

⁴ Facultad de Ingeniería en Electricidad y Computación, Escuela Superior Politécnica del Litoral, ESPOL, Campus Gustavo Galindo Km 30.5 Vía Perimetral, P.O. Box 09-01-5863, 090150 Guayaquil, Ecuador

⁵ Department of Automation, Technical University of Cluj-Napoca, Memorandumului Street No.28, Cluj-Napoca 400114, Romania

* Correspondence: Shiquan.Zhao@ugent.be

Received: 11 March 2020; Accepted: 7 April 2020; Published: 11 April 2020



Abstract: The steam/water loop is a crucial part of a steam power plant. However, satisfying control performance is difficult to obtain due to the frequent disturbance and load fluctuation. A fractional order model predictive control was studied in this paper to improve the control performance of the steam/water loop. Firstly, the dynamic of the steam/water loop was introduced in large-scale ships. Then, the model predictive control with an extended prediction self adaptive controller framework was designed for the steam/water loop with a distributed scheme. Instead of an integer cost function, a fractional order cost function was applied in the model predictive control optimization step. The superiority of the fractional order model predictive control was validated with reference tracking and load fluctuation experiments.

Keywords: multi-input multi-output system; steam power plant; fractional order; model predictive control; large scale ships

1. Introduction

A total of 80% trade volume is moved with shipping industry, which is becoming an important part of the world economy [1]. In order to obtain large carrying capacity and low operation cost, there is a large demand for large-scale cargo ships. To achieve energy saving and a stable energy supply, research is required to optimize the power plant in large-scale ships [2]. The steam/water loop in large scale ships has the function of supplying water and recovering the waste steam for the steam power plant. There are five output variables including the drum water level, exhaust manifold pressure, deaerator pressure, deaerator water level and condenser water level. The steam/water loop has the features of nonlinearity, multi variables and strong coupling system. During the operating of the ship, the frequent disturbance and load fluctuation make it difficult to obtain a satisfying control effect for the five sub-loops [3]. The challenges in the control of steam/water loop can be summarized as follows:

- the steam/water loop is a system of nonlinearity, strong interactions and multivariable;
- load and disturbances change frequently with large amplitude;
- operating conditions changes frequently (there are ten levels of the sea state);
- demands for mobility and rapidity are growing high.

The Model Predictive Control (MPC) is a widely applied controller in industrial processes for its ability to deal with constraints such as the input saturation and rate limits. The dynamic model of the system is required to predict and optimize the future error and control effort by minimizing a cost function [4]. MPC has become the mostly applied control strategy in a wide variety of areas, including petroleum, refining and chemical industries [5]. Part of the work about the application of MPC to the boiler system is shown in [6–8]. In the cost function, an economic index was included [6]. The reference tracking and the economic performance were both realized. To realize satisfying control performance for ultra-supercritical boiler, a fuzzy model was obtained for the fuzzy MPC, and a linear extended state observer was improved to estimate plant behavior variations and unknown disturbances [7]. A state-space model was linearized on-line to improve the computationally efficient in model predictive control, and the results were similar to the results obtained with nonlinear model [8]. For tuning the closed loops with MPC, a practical method with step response of the system was proposed [9]. The methodology is suitable for hands-on tuning of MPC. Compared with PID control, it is discussed about when, where and why to apply the MPC with the advent of Industry 4.0 [10].

The fractional order calculus has attracted increasing attention over the past two decades for its versatility in modeling and control applications [11]. Although the computational load will increase with fractional order, nowadays, the development of microprocessor makes it possible for such kind of computation. Some types of control strategies have been generalized with fractional order calculus [12,13]. For example, the PID controller is the most used in industry [14], hence, fractional order calculation was added to PID controller in many applications such as: AR.Drone quad-rotor [15], induction motor drive system [16], multi-area interconnected power systems [17], heterogeneous dynamic systems [18], automatic regulator voltage system [19], multiple UAVs formation [20,21], velocity control system [22]. The fractional order calculus is also applied in the MPC method. And the application can be found such as temperature control [23], and frequency control of an islanded micro-grid [24].

In the fractional order calculus, ${}_a D_b^\alpha$ is commonly used for α -th order derivative in the interval $[a, b]$, and ${}_a I_b^\alpha$ the α -th fractional order integral in the interval $[a, b]$. There are two kinds of approximate estimators for the fractional calculus. One is the Grünwald-Letnikov (GL) definition, and another Riemann-Liouville (RL) definition. The RL definition is used for continuous domain, while GL definition for numerical integration and simulation purposes. Their definitions are

$${}_a D_t^\alpha f(t)_{t=kT_s} = \lim_{T_s \rightarrow 0} T_s^{-\alpha} \sum_{i=0}^{\lfloor \frac{t-a}{T_s} \rfloor} (-1)^i \binom{\alpha}{i} f(kT_s - iT_s) \quad \text{GL} \quad (1)$$

$${}_a D_t^\alpha f(t) = \frac{1}{\Gamma(n-\alpha)} \frac{d^n}{dt^n} \int_a^t \frac{f(\tau)}{(t-\tau)^{(\alpha-n+1)}} d\tau \quad \text{RL} \quad (2)$$

where T_s is the sampling time and $\Gamma(\cdot)$ is Euler's Gamma function.

In this paper, the original contribution lies in that the constant values of the weighting factors in classical MPC is replaced with time-varying weighting factors in fractional order MPC (FOMPC). The weight factors in the classical MPC have $N_p + N_c$ elements for tracking error and control effort need to be defined, where N_p is prediction horizon and N_c is control horizon. The optimal problem for the weighting factors will be very complex. Hence, the weighting factors are mostly kept as constants in MPC. In the FOMPC, the weighting factors are obtained with the fractional orders, in which optimal different weighting factors can be tuned with two fractional orders, one for the tracking error and another for control effort. Hence, the FOMPC will result in a better system performance than the MPC method. In this work, fractional order MPC is proposed firstly for steam/water loop with GL definition. Then, the integer order cost function is replaced with a fractional order one in the MPC. In order to obtain a relatively good value set for the five sub-loops, different fractional orders are required for each sub-loop. The results show that the bigger fractional order leads to better control

performance. Finally, reference tracking and load fluctuation experiments are conducted to verify the effectiveness of the FOMPC.

The paper is structured as follows: firstly, the steam/water loop is introduced in Section 2. Section 3 gives a brief introduction about Extended Prediction Self Adaptive Controller (EPSAC), and the fractional order cost function is designed. Section 4 shows the results of FOMPC compared with classical MPC. Conclusions are discussed in Section 5.

2. The Description for Steam/Water Loop

The steam/water loop in the large scale ships plays the role of supplying water to the boiler and recycling waste steam from turbine. The system is composed of a boiler drum, exhaust manifold, deaerator and condenser. The system operating principle can be found in Figure 1, in which there are two main operating loops. One is indicated with the red line for the steam loop, while the green line for the water loop. The description for the system are as follows: firstly, the condensed water from condenser goes to the deaerator for preheating and deoxygenation. Secondly, the feedwater is pumped to the drum. Due to the high density of the water than the steam, the water goes to the mud-drum. In the risers, the water absorbs the heat and becomes the mixture of steam and water. The steam gets separated in the drum and goes to the turbine after being heated in the economizer. The waste steam from the turbine and other auxiliary machines goes to the exhaust manifold. Most of the waste steam goes to the condenser, and the left part of waste steam goes to the deaerator for deoxygenation. Finally, the condensate water goes to the deaerator to work again.

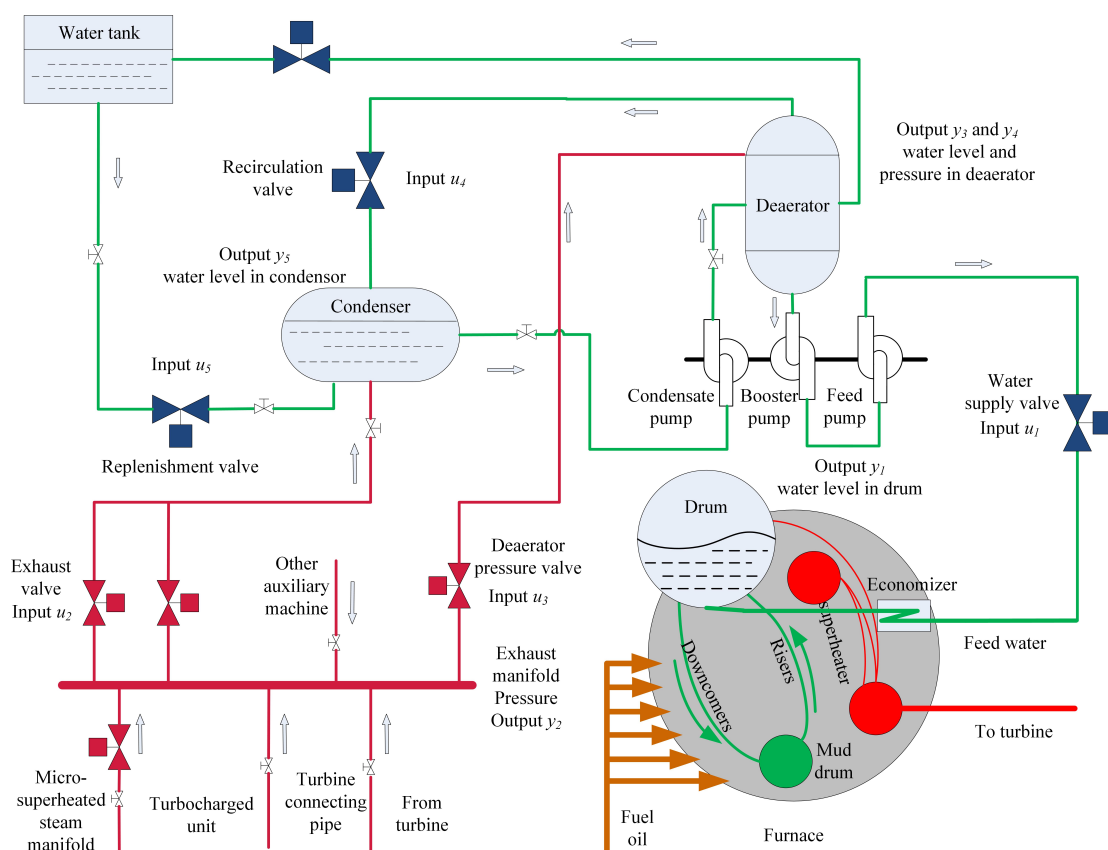


Figure 1. Structure of the steam/water loop [25] (reproduced with permission from Zhao, S.; Maxim, A.; Liu, S.; De Keyser, R.; and Ionescu, C, Processes; published by MDPI, 2018.).

In the steam/water loop, the input variables $\mathbf{u} = [u_1, u_2, \dots, u_5]$ are valves for the five sub-loops, and the output variables $\mathbf{y} = [y_1, y_2, \dots, y_5]$ are the drum water level (y_1), exhaust manifold pressure

(y_2), deaerator pressure (y_3), deaerator water level (y_4), and condenser water level (y_5), respectively [3]. The transfer functions and constraints of the steam/water loop are shown as follows:

$$\begin{bmatrix} y_1 \\ y_2 \\ \vdots \\ y_5 \end{bmatrix} = \begin{bmatrix} G_{11} & G_{12} & \cdots & G_{15} \\ G_{21} & G_{22} & \cdots & G_{25} \\ \vdots & \vdots & \ddots & \vdots \\ G_{51} & G_{52} & \cdots & G_{55} \end{bmatrix} \begin{bmatrix} u_1 \\ u_2 \\ \vdots \\ u_5 \end{bmatrix} \quad (3)$$

where $G_{11} = \frac{0.0000987}{(s+0.1131)(s+0.0085+0.032j)(s+0.0085-0.032j)}$, $G_{22} = \frac{0.7254}{(s+1.2497)(s+0.0223)}$,
 $G_{23} = \frac{-0.5}{(s+1.9747)(s+0.0253)}$, $G_{33} = \frac{0.0132}{(s+0.0265+0.0244j)(s+0.0265-0.0244j)}$, $G_{34} = \frac{-0.009}{(s+0.0997)(s+0.0411)}$,
 $G_{41} = \frac{-0.0008}{(s+0.012+0.126j)(s+0.012-0.126j)}$, $G_{44} = \frac{0.0005152}{(s+0.012+0.038j)(s+0.012-0.038j)}$,
 $G_{54} = \frac{-0.00015}{(s+0.0175+0.0179j)(s+0.0175-0.0179j)}$, $G_{55} = \frac{0.00147}{(s+0.025+0.0654j)(s+0.025-0.0654j)}$, and other transfer functions $G_{12} = G_{13} = \dots = G_{53} = 0$.

$$\left\{ \begin{array}{l} -0.007/s \leq \frac{du_1}{dt} \leq 0.007/s \quad 0 \leq u_1 \leq 1 \\ -0.01/s \leq \frac{du_2}{dt} \leq 0.01/s \quad 0 \leq u_2 \leq 1 \\ -0.01/s \leq \frac{du_3}{dt} \leq 0.01/s \quad 0 \leq u_3 \leq 1 \\ -0.007/s \leq \frac{du_4}{dt} \leq 0.007/s \quad 0 \leq u_4 \leq 1 \\ -0.007/s \leq \frac{du_5}{dt} \leq 0.007/s \quad 0 \leq u_5 \leq 1 \end{array} \right. \quad (4)$$

The operating point and ranges of variables are shown in Table 1.

Table 1. The operating points and range of the steam/water loop.

Outputs	Operating Points	Range	Units
Water level in drum	1.79	[1.39–2.19]	m
Pressure in exhaust manifold	100.03	[87.03–133.8]	MPa
Pressure in deaerator	30	[24.9–43.86]	KPa
Water level in deaerator	0.7	[0.49–0.89]	m
Water level in condenser	0.5	[0.32–0.63]	m

3. Fractional Order MPC with EPSAC Framework

3.1. Brief Introduction for EPSAC

In this part, a brief introduction about EPSAC is given, and the detailed theory is introduced in [26]. For a discrete system:

$$y(t) = x(t) + w(t) \quad (5)$$

where t is the discrete time index; $y(t)$ and $x(t)$ are the system output and model output, respectively; and $w(t)$ indicates the disturbance. The model output $x(t)$ can be obtained according to the system model and past model outputs and inputs:

$$x(t) = f[x(t-1), x(t-2), \dots, u(t-1), u(t-2), \dots] \quad (6)$$

The following two parts compose the future input in EPSAC:

$$u(t+k|t) = u_{base}(t+k|t) + \delta u(t+k|t) \quad (7)$$

where the $u_{base}(t+k|t)$ indicates the basic future control actions and $\delta u(t+k|t)$ is the optimized future control actions. With these two parts of future input, the predicted future system output can be divided with the following two parts:

$$y(t+k|t) = y_{base}(t+k|t) + y_{opt}(t+k|t) \quad (8)$$

where $y_{base}(t+k|t)$ is produced with the basic future control action $u_{base}(t+k|t)$ and $y_{opt}(t+k|t)$ is obtained with optimized future control action $\delta u(t+k|t)$. According to the discrete input scenario, the $y_{opt}(t+k|t)$ can be obtained with:

$$y_{opt}(t+k|t) = h_k \delta u(t|t) + h_{k-1} \delta u(t+1|t) + \dots + g_{k-N_c+1} \delta u(t+N_c-1|t) \quad (9)$$

where the h_i and g_i are the impulse response and step response coefficients of the system; N_c is the control horizon and N_p the prediction horizon. The system output can be re-written as:

$$\mathbf{Y} = \bar{\mathbf{Y}} + \mathbf{G}\mathbf{U} \quad (10)$$

with $\mathbf{Y} = [y(t+N_1|t) \dots y(t+N_p|t)]^T$, $\mathbf{U} = [\delta u(t|t) \dots \delta u(t+N_c-1|t)]^T$, $\bar{\mathbf{Y}} = [y_{base}(t+N_1|t) \dots y_{base}(t+N_p|t)]^T$, and

$$\mathbf{G} = \begin{bmatrix} h_{N_1} & h_{N_1-1} & \dots & g_{N_1-N_c+1} \\ h_{N_1+1} & h_{N_1} & \dots & \dots \\ \dots & \dots & \dots & \dots \\ h_{N_p} & h_{N_p-1} & \dots & g_{N_p-N_c+1} \end{bmatrix}$$

where N_1 is the time delay of the system.

The disturbance term $w(t)$ in Equation (5) is taken as a filtered white noise [26], which is given by:

$$w(t+k|t) = \frac{C(q^{-1})}{D(q^{-1})} w_f(t+k|t) \quad (11)$$

where q^{-1} is the backward shift operator; $D(q^{-1}) = (1 - q^{-1})A(q^{-1})$; and $A(q^{-1})$, $C(q^{-1})$ are polynomials from Controlled Auto-Regressive Integrated Moving Average (CARIMA) model.

The cost function gives:

$$J_{MPC} = \sum_{k=N_1}^{N_p} p_k [r(t+k|t) - y(t+k|t)]^2 + \sum_{k=1}^{N_u} q_k \Delta u(t+k)^2 \quad (12)$$

where p_k and q_k are nonnegative weighting factors, which are kept as constants.

Rewrite the Equation (12) into matrix form, and the following can be obtained:

$$J_{MPC} = (\mathbf{R} - \mathbf{Y})^T \mathbf{P} (\mathbf{R} - \mathbf{Y}) + \mathbf{U}^T \mathbf{Q} \mathbf{U} = (\mathbf{R} - \bar{\mathbf{Y}} - \mathbf{G}\mathbf{U})^T \mathbf{P} (\mathbf{R} - \bar{\mathbf{Y}} - \mathbf{G}\mathbf{U}) + \mathbf{U}^T \mathbf{Q} \mathbf{U} \quad (13)$$

where $P = \text{diag}(p_1, p_2, \dots, p_{(N_p - N_1 + 1)})$ and $Q = \text{diag}(q_1, q_2, \dots, q_{N_u})$.

If there are constraints in the optimization problem, it can be solved with quadratic programming. Without constraints, the optimal input sequence for $\delta u(t + k|t)$ gives:

$$\mathbf{U}_{\text{MPC}}^* = (\mathbf{G}^T \mathbf{P} \mathbf{G} + \mathbf{Q})^{-1} \mathbf{G}^T \mathbf{P} (\mathbf{R} - \tilde{\mathbf{Y}}) \quad (14)$$

For the fractional order MPC, the cost function can be expressed with

$$J_{\text{FOMPC}} = {}^\gamma I_{N_1}^{N_p} p_k [r(t + k|t) - y(t + k|t)]^2 + {}^\lambda I_1^{N_c} q_k \Delta u(t + k)^2 \quad (15)$$

where $[N_1, N_p]$ and $[1, N_c]$ are the integration intervals, and ${}^\gamma I_{N_1}^{N_p}$ and ${}^\lambda I_1^{N_c}$ are the symbols for fractional order integral with γ and λ the fractional orders. The ${}^\gamma I_{N_1}^{N_p}$ and ${}^\lambda I_1^{N_c}$ can be rewritten as:

$$\begin{aligned} {}^\gamma I_{N_1}^{N_p} p_k [r(t + k|t) - y(t + k|t)]^2 &= \int_{N_1}^{N_p} D^{1-\gamma} p_k [r(t + k|t) - y(t + k|t)]^2 dt \\ {}^\lambda I_1^{N_c} q_k \Delta u(t + k)^2 &= \int_{N_1}^{N_c} D^{1-\lambda} q_k \Delta u(t + k)^2 dt \end{aligned} \quad (16)$$

According to [27], the Equation (15) can be approximated by:

$$\begin{aligned} J_{\text{FOMPC}} &= (\mathbf{R} - \mathbf{Y})^T \mathbf{P} \mathbf{\Gamma}(T_s, \gamma) (\mathbf{R} - \mathbf{Y}) + \mathbf{U}^T \mathbf{Q} \mathbf{\Lambda}(T_s, \lambda) \mathbf{U} \\ &= (\mathbf{R} - \tilde{\mathbf{Y}} - \mathbf{G} \mathbf{U})^T \mathbf{P} \mathbf{\Gamma}(T_s, \gamma) (\mathbf{R} - \tilde{\mathbf{Y}} - \mathbf{G} \mathbf{U}) + \mathbf{U}^T \mathbf{Q} \mathbf{\Lambda}(T_s, \lambda) \mathbf{U} \end{aligned} \quad (17)$$

$$\mathbf{\Gamma}(T_s, \gamma) = T_s^\gamma \text{diag}(m_{N_p - N_1}, m_{N_p - N_1 - 1}, \dots, m_1, m_0) \quad (18)$$

$$\mathbf{\Lambda}(T_s, \lambda) = T_s^\lambda \text{diag}(m_{N_c}, m_{N_c - 1}, \dots, m_1, m_0) \quad (19)$$

The m_i with fractional order α gives:

$$m_j = \omega_j^{(-\alpha)} - \omega_{j-n}^{(-\alpha)} \quad (20)$$

where n is the number of the m_i .

$$\omega_j^{-\alpha} = \begin{cases} (1 - (1 - \alpha)/j) \omega_{j-1}^{(-\alpha)} & j > 0; \\ 1 & j = 0; \\ 0 & j < 0. \end{cases} \quad (21)$$

From Equation (18) to Equation (21), the weight matrix can be easily tuned with fractional order γ and λ in the cost function J_{FOMPC} . And the weighting factors in the FOMPC are time-varying along the prediction horizon and control horizon. If there are constraints, the optimization problem can be solved with quadratic programming. Without constraints, the optimal input sequence for $\delta u(t + k|t)$ in FOMPC can be obtained as:

$$\mathbf{U}_{\text{FOMPC}}^* = (\mathbf{G}^T \mathbf{P} (\mathbf{\Gamma} + \mathbf{\Gamma}^T) \mathbf{G} + \mathbf{Q} (\mathbf{\Lambda} + \mathbf{\Lambda}^T))^{-1} \mathbf{G}^T \mathbf{P} (\mathbf{\Gamma} + \mathbf{\Gamma}^T) (\mathbf{R} - \tilde{\mathbf{Y}}) \quad (22)$$

3.2. Applied the EPSAC to the MIMO System with Distributed Scheme

Due to the flexibility and robustness of the distributed control, the EPSAC is applied to the steam/water loop in distributed scheme, in which each sub-loop works as independent modules with communication network. The application of distributed fractional order MPC on the steam/water loop is similar to the method introduced in [3], and the integer cost function is replaced with fractional order cost function. Only a brief introduction is given here about the distributed MPC.

In the distributed MPC, the inference from other sub-loops should be considered to optimize the future error and control effort for sub-loop i , hence, the item \mathbf{GU} in Equations (13) and (17) should be replaced with $\sum_{j=1}^5 \mathbf{G}_{ij} \mathbf{U}_j$, and \mathbf{G}_{ij} is the transfer function of i^{th} output from j^{th} input. A pseudo-code for the distributed MPC is provided in Algorithm 1.

Algorithm 1 The iterative DiMPC

- 1: Sub-loop i receives an optimal local control action $\delta \mathbf{U}_i$ at the iterative time as $iter = 0$ according to the EPSAC, and the local control action $\delta \mathbf{U}_i$ can be marked as $\delta \mathbf{U}_i^{iter}$, where $\delta \mathbf{U}_i$ indicates the vector of the optimizing future control actions with length of N_{ci} ;
 - 2: The $\delta \mathbf{U}_j^{iter}$ ($j \in N_i$, $N_i = \{j \in N : \mathbf{G}_{ij} \neq 0\}$) will be communicated with the loop i , and the $\delta \mathbf{U}_i^{iter+1}$ will be calculated again with the $\delta \mathbf{U}_j^{iter}$ from other loops;
 - 3: If one of the termination conditions is reached, the $\delta \mathbf{U}_i^{iter+1}$ will be adopted to the system. Otherwise, the $iter$ will be set as $iter = iter + 1$, and return to Step 2. The termination condition is shown as follows: $(\|\delta \mathbf{U}_i^{iter+1} - \delta \mathbf{U}_i^{iter}\| \leq \varepsilon_i) \vee (iter + 1 > \overline{iter})$, where ε is a positive constant and \overline{iter} indicates the upper bound of the number of iteration times.
 - 4: Calculate the optimal control effort as $\mathbf{U}_t = \mathbf{U}_{base} + \delta \mathbf{U}^{iter}$, and the control effort will be applied to the system;
 - 5: Set $t = t + 1$, return to Step 1.
-

4. Results and Discussion

In this paper, reference tracking and load fluctuation experiments are conducted to verify the effectiveness of the FOMPC. The parameter configuration is listed in Table 2.

Table 2. MPC parameters.

Parameters	N_c	T_s	N_p	N_1	N_s
Values	$N_{c1} = 4, N_{c2} = 1,$ $N_{c3} = 1, N_{c4} = 4,$ $N_{c5} = 6$ samples	5s	$N_{p1} = 20, N_{p2} = 15,$ $N_{p3} = 15, N_{p4} = 20,$ $N_{p5} = 20$ samples	1	300

where, N_s is the number of samples. The termination conditions for the distributed MPC are set as: (i) $\|\delta \mathbf{U}_i^{iter+1} - \delta \mathbf{U}_i^{iter}\| \leq 0.002$; (ii) $iter > 5$.

4.1. The Effect of Different Fractional Orders on the Overall System Performance

The choice of fractional orders of γ and λ have important influence on the system. To explore the effect of different fractional orders, the fractional orders listed in Table 3 are applied for each sub-loop.

Table 3. Different fractional orders for the five sub-loops.

Loops	Fractional Orders
Drum water level control loop	[6.2 5.0 3.8 2.6 1.0 0.8]
Exhaust manifold pressure control loop	[1.2 1.0 0.9 0.62 0.36 0.12]
Deaerator pressure control loop	[5.0 3.8 2.2 1.4 1.0 0.6]
Deaerator water level control loop	[1.5 1.2 1.0 0.8 0.4]
Condenser water level control loop	[2.2 1.8 1.2 1.0 0.7 0.3]

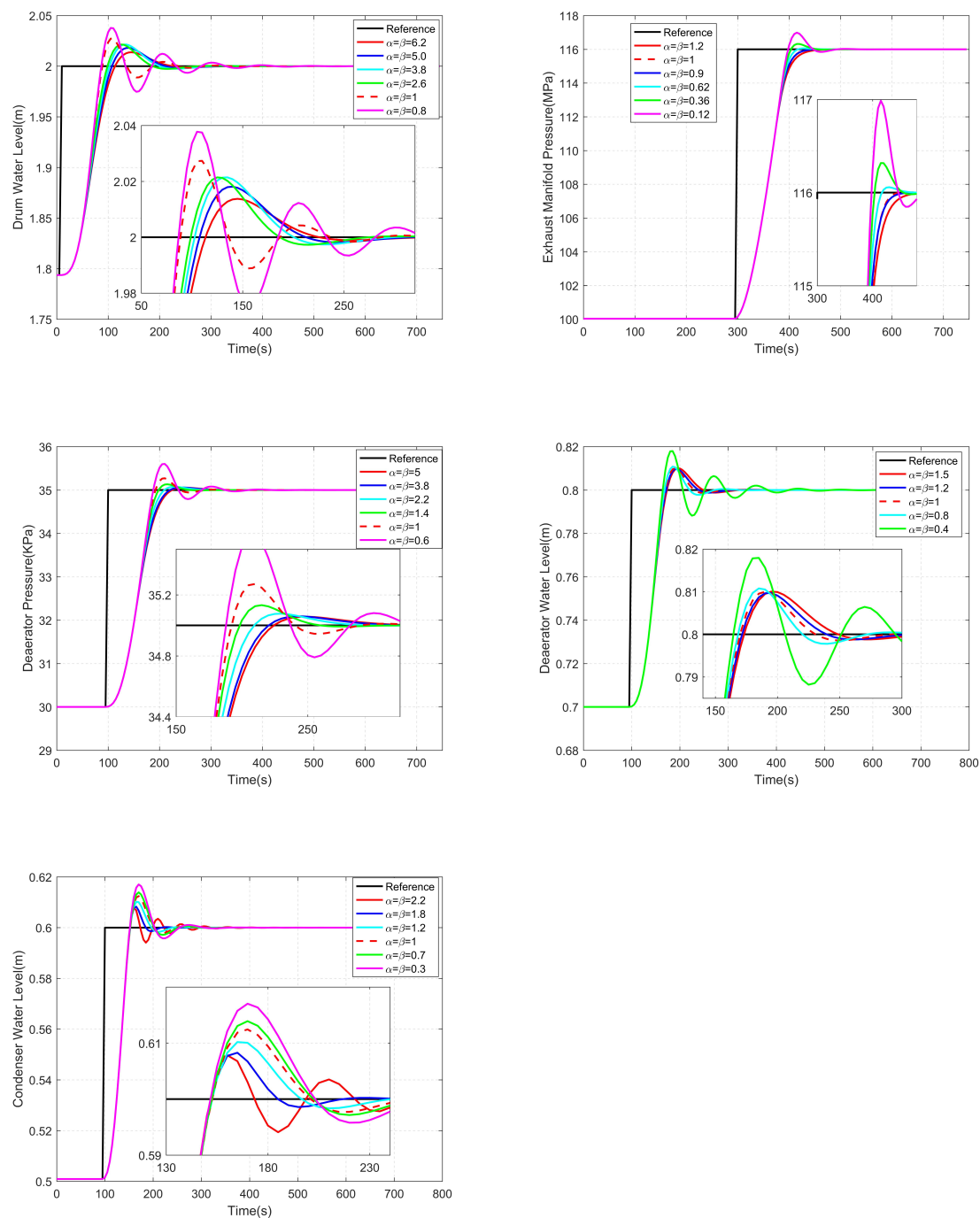


Figure 2. Outputs with different fractional orders for the five sub-loops.

Intuitively from the results shown in Figure 2, all the outputs of the five sub-loops indicate that the larger fractional order leads to better responses both in response time and overshoot in a certain range. Also, the overshoot reduces with large fractional order value.

4.2. Reference Tracking Performance

According to the results from previous section, The fractional orders for the five sub-loops are chosen as 6.2, 0.62, 2.2, 1.2 and 1.2, respectively. The following indexes are applied to evaluate the performance of the FOMPC and MPC, including the Integrated Absolute Relative Error (IARE),

Integral Secondary control output (ISU), Ratio of Integrated Absolute Relative Error ($RIARE$), Ratio of Integral Secondary control output ($RISU$) and combined index (J).

$$IARE_i = \sum_{k=0}^{N_s-1} |r_i(k) - y_i(k)| / r_i(k) \quad (i = 1, 2, \dots, 5) \quad (23)$$

$$ISU_i = \sum_{k=0}^{N_s-1} (u_i(k) - u_{ssi}(k))^2 \quad (i = 1, 2, \dots, 5) \quad (24)$$

$$RIARE_i(C_2, C_1) = \frac{IARE_i(C_2)}{IARE_i(C_1)} \quad (i = 1, 2, \dots, 5) \quad (25)$$

$$RISU_i(C_2, C_1) = \frac{ISU_i(C_2)}{ISU_i(C_1)} \quad (i = 1, 2, \dots, 5) \quad (26)$$

$$J(C_2, C_1) = \frac{1}{5} \sum_{i=1}^5 \frac{w_1 RIARE_i(C_2, C_1) + w_2 RISU_i(C_2, C_1)}{w_1 + w_2} \quad (27)$$

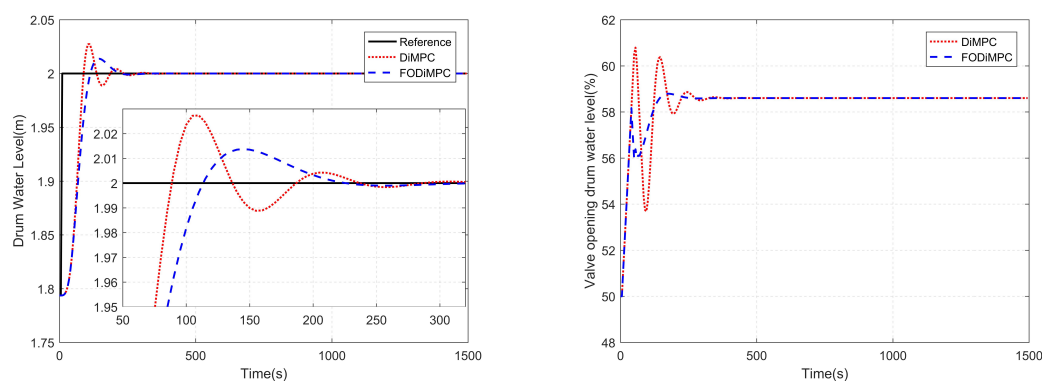
where u_{ssi} is the steady state value of i^{th} input; C_1, C_2 are the two compared controllers; the weighting factors w_1 and w_2 in equation (27) are chosen as $w_1 = w_2 = 0.5$.

In the Reference tracking experiment, step signals are introduced to the system at different time. The setpoints for the five loops are shown in Table 4.

Table 4. Setpoints for different loops in the experiments.

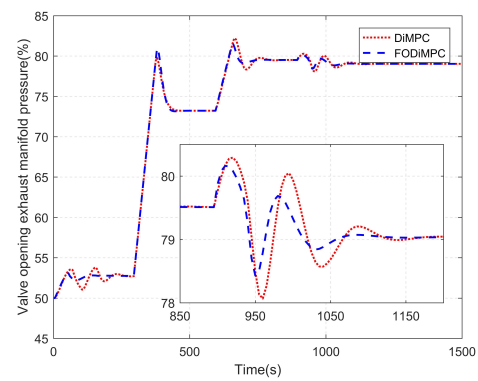
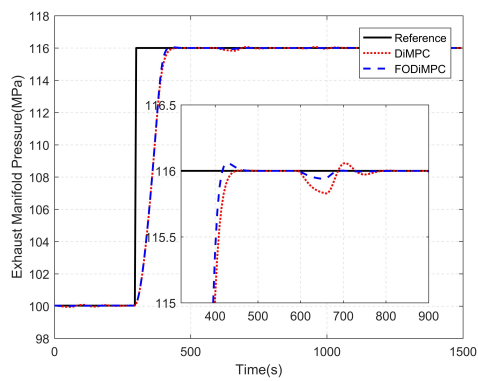
Time (s)	2–300	300–600	600–900	900–1200	1200–1500
Drum Water Level (m)	2	2	2	2	2
Exhaust Manifold Pressure(MPa)	100.03	116	116	116	116
Deaerator Pressure (KPa)	30	30	35	35	35
Deaerator Water Level(m)	0.7	0.7	0.7	0.8	0.8
Condenser Water Level(m)	0.5	0.5	0.5	0.5	0.6

The simulation results about reference tracking performance are shown in Figure 3. And the performance indexes are shown in Tables 5 and 6.

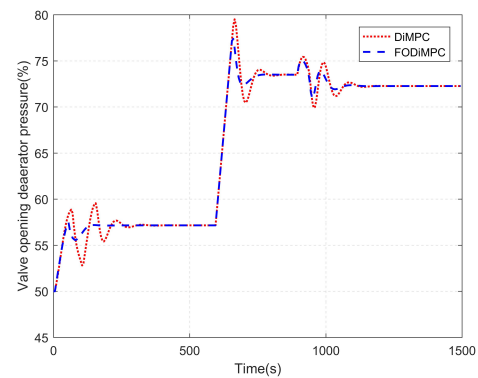
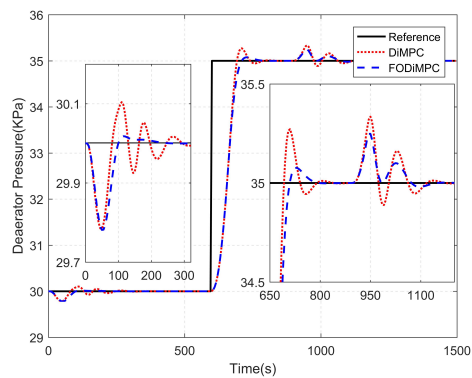


(a) drum water level control loop

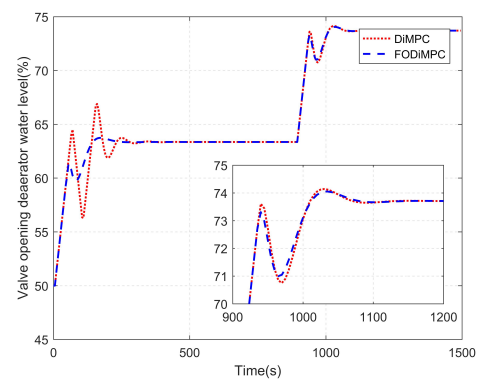
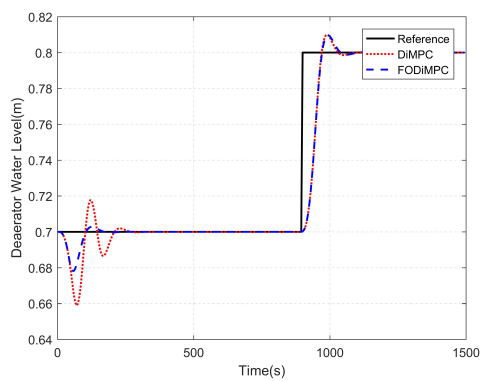
Figure 3. Cont.



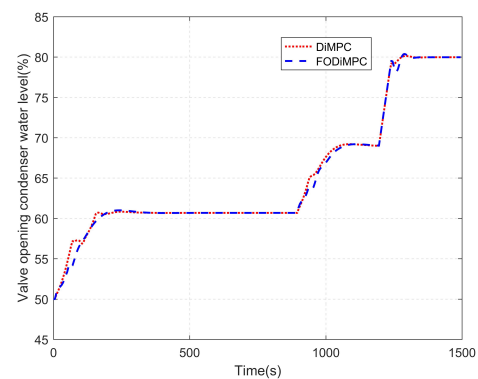
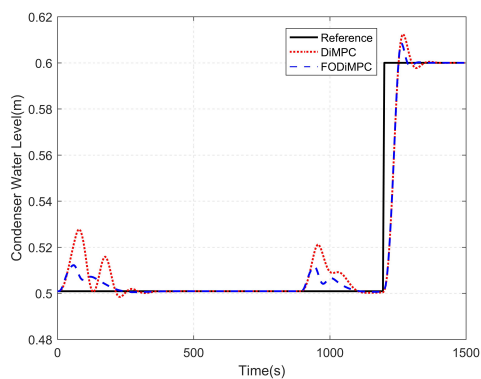
(b) exhaust manifold pressure control loop



(c) deaerator pressure control loop



(d) deaerator water level control loop



(e) condenser water level control loop

Figure 3. Outputs of the steam/water loop with FOMPC and MPC in the reference tracking experiment (The outputs are listed on the left hand, and the inputs are listed on the right hand).

Table 5. Indexes for *IARE* and *ISU* in the reference tracking experiment.

Index		Loop 1	Loop 2	Loop 3	loop 4	Loop 5
<i>IARE</i>	MPC	1.2614	1.6972	1.9464	2.0500	2.9060
	FOMPC	1.3337	1.6411	1.8813	1.5570	1.9686
<i>ISU</i>	MPC	0.0302	0.4776	0.1330	0.1577	1.6925
	FOMPC	0.0205	0.4719	0.1014	0.1371	1.7689

Table 6. Indexes for *RIARE* and *RISU* in the reference tracking experiment (MPC is the C_2 and FOMPC the C_1 according to Equations (25) and (26)).

Index	Loop 1	Loop 2	Loop 3	Loop 4	Loop 5
<i>RIARE</i>	0.9458	1.0342	1.0346	1.3166	1.4762
<i>RISU</i>	1.4729	1.0119	1.3119	1.1503	0.9568

The combined index J for the reference tracking case is 1.1711. Both from the Figure 3 and performance indexes, it can be concluded that the FOMPC outperforms the MPC in reference tracking experiment. The response time and overshoot are both smaller in FOMPC than those in the traditional MPC. From Table 5, the *ISUs* for sub-loop 5 are similar, however, the *IAREs* are much different from each other. This is caused by the interaction between water levels of deaerator and condenser water level. The condenser has a smaller volume than the deaerator, hence, the water level in condenser changes a lot along with the deaerator water level.

4.3. Load Disturbance Rejection Performance

In the simulation of the load disturbance rejection experiment, 20% load increase from time period 100 s to 150 s and 20% load decrease from time period 850 s to 900 s are introduced in the steam/water loop. And the simulation results for load disturbance rejection experiment are shown in Figure 4 and Tables 7 and 8.

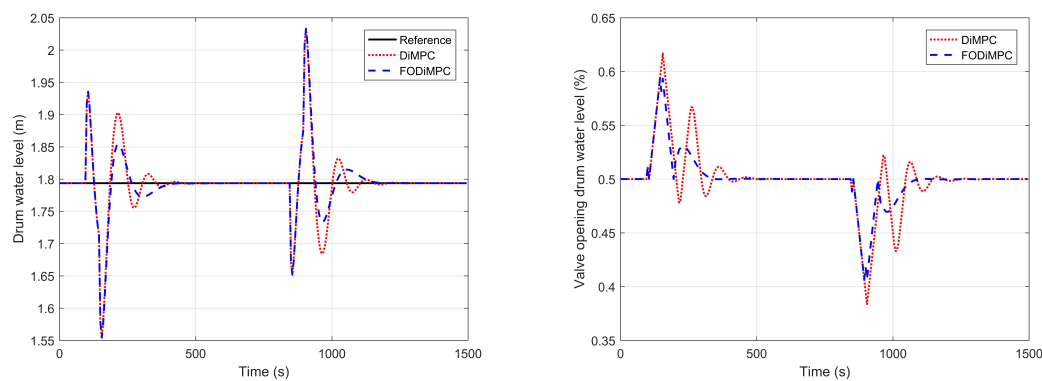
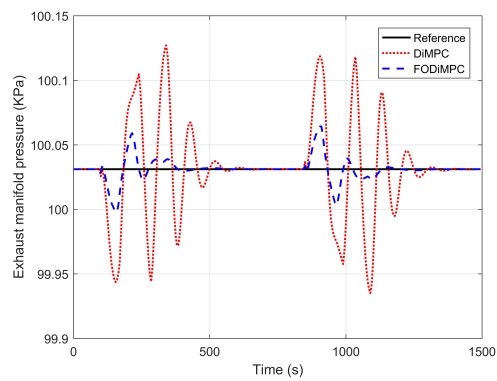
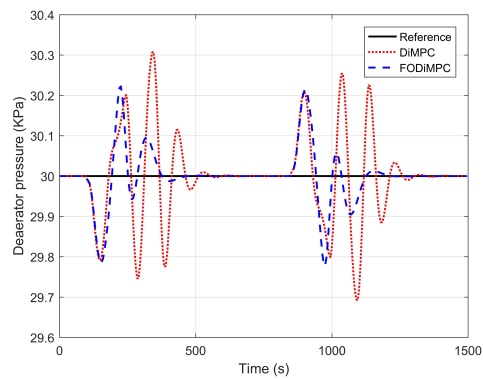
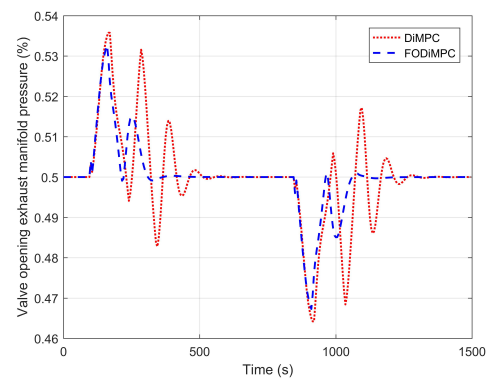
**(a)** drum water level control loop

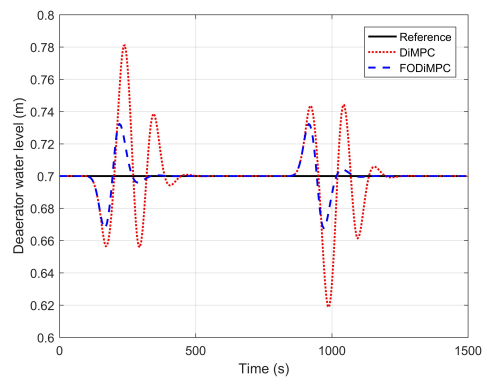
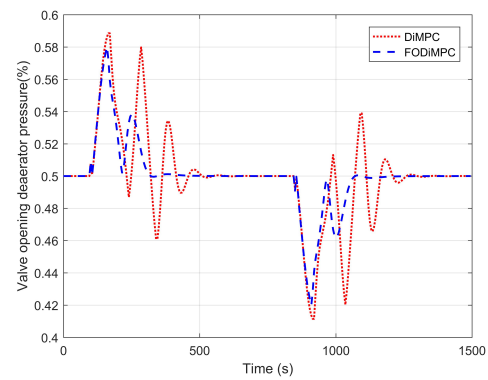
Figure 4. Cont.



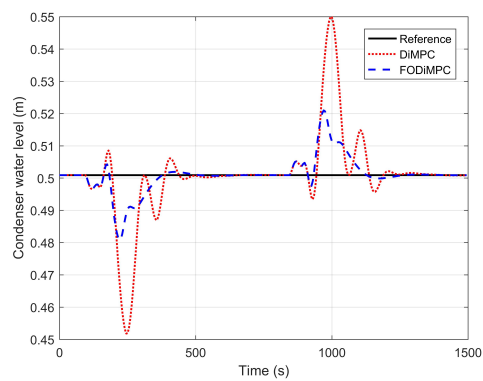
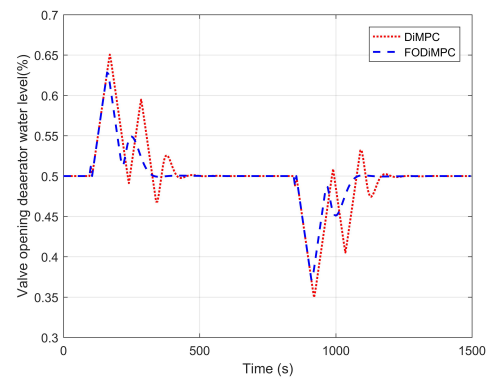
(b) exhaust manifold pressure control loop



(c) deaerator pressure control loop



(d) deaerator water level control loop



(e) condenser water level control loop

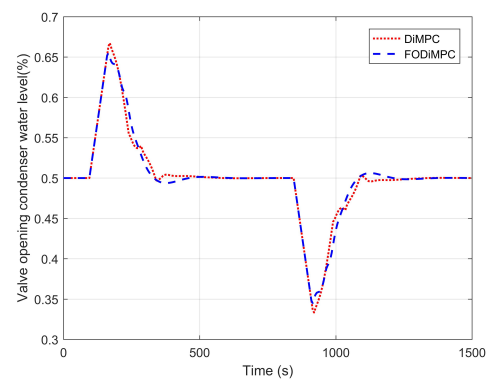


Figure 4. Outputs variables with FOMPC and MPC in the load fluctuation experiment (The outputs are listed on the left hand, and the inputs are listed on the right hand).

Table 7. Indexes for *IARE* and *ISU* in the load fluctuation experiment.

Index		Loop 1	Loop 2	Loop 3	Loop 4	Loop 5
<i>IARE</i>	MPC	3.5312	0.0686	0.6469	4.8710	3.4694
	FOMPC	3.1523	0.0129	0.3402	1.6632	1.6197
<i>ISU</i>	MPC	0.2403	0.0393	0.2379	0.5215	0.7876
	FOMPC	0.1452	0.0206	0.1253	0.3114	0.7855

Table 8. Indexes for *RIARE* and *RISU* in the load fluctuation experiment (MPC is the C_2 and FOMPC the C_1 according to Equations (25) and (26)).

Index	Loop 1	Loop 2	Loop 3	Loop 4	Loop 5
<i>RIARE</i>	1.1202	5.3201	1.9016	2.9287	2.1420
<i>RISU</i>	1.6551	1.9049	1.8988	1.6748	1.0027

The combined index J for the load fluctuation case is 2.1549. Compared with MPC, the FOMPC method reduces the tracking error by 168%, and reduces the amount of control effort changes by 62.7%. The FOMPC has a significant improvement than the MPC method. With less control effort, the FOMPC can achieve better load disturbance rejection performance than the MPC.

5. Conclusions

By replacing the integer cost function with a fractional order one, the fractional order MPC based on EPSAC framework is applied to the steam/water loop in large scale ships. The comparison between FOMPC and MPC shows the FOMPC has better performance both in the reference tracking and load disturbance rejection. Different fractional orders are applied to the five sub-loops in steam/water loop, and it is concluded that within a certain range of the fractional order, the larger the order leads to better performance.

Author Contributions: methodology, R.D.K., C.-M.I. and S.Z.; software, S.Z. and R.C.; formal analysis, S.Z.; writing—original draft preparation, S.Z.; writing—review and editing, S. Z., R.C., R.D.K. and C.-M.I.; supervision, C.-M.I. and R.D.K.; funding acquisition, S.Z. and C.-M.I. All authors have read and agreed to the published version of the manuscript

Funding: C.-M.I. gratefully acknowledges the financial support for this work from Ghent University Special Research Fund, project MIMOPREC—Starting grant 2018. R.C. received in part funding from Flanders Make—CONACON project nr HBC.2018.0235. R.C. gratefully acknowledges the financial support from ESPOL and National Secretariat of Higher Education, Science, Technology and Innovation of Ecuador (SENESCYT). Part of this project is funded by National Natural Science Foundation of China subsidization project (51579047), the Doctoral Scientific Research Foundation of Heilongjiang (No. LBH-Q14040), the Fundamental Research Funds for the Central Universities under grant 3072019CF0408, 3072019CFT0403.

Acknowledgments: Mr Shiquan Zhao acknowledges the financial support from Chinese Scholarship Council (CSC) under grant 201706680021 and the Co-funding for Chinese PhD candidates from Ghent University under grant 01SC1918.

Conflicts of Interest: The authors declare no conflict of interest.

References

1. Lamnabhi-Lagarigue, F.; Annaswamy, A.; Engell, S.; Isaksson, A.; Khargonekar, P.; Murray, R.M.; Nijmeijer, H.; Samad, T.; Tilbury, D.; Van den Hof, P. Systems & Control for the future of humanity, research agenda: Current and future roles, impact and grand challenges. *Annu. Rev. Control* **2017**, *43*, 1–64.
2. Drbal, L.; Westra, K.; Boston, P. *Power Plant Engineering*; Springer Science & Business Media: Berlin, Germany, 2012.

3. Zhao, S.; Maxim, A.; Liu, S.; De Keyser, R.; Ionescu, C.M. Distributed model predictive control of steam/water loop in large scale ships. *Processes* **2019**, *7*, 442.
4. Romero, M.; Mañoso, C.; Ángel, P.; Vinagre, B.M. Fractional-order generalized predictive control: Formulation and some properties. In Proceedings of the 2010 11th International Conference on Control Automation Robotics & Vision, Singapore, 7–10 December 2010; pp. 1495–1500.
5. Samad, T. A survey on industry impact and challenges thereof [technical activities]. *IEEE Control Syst. Mag.* **2017**, *37*, 17–18.
6. Liu, X.; Cui, J. Economic model predictive control of boiler-turbine system. *J. Process Control* **2018**, *66*, 59–67.
7. Zhang, F.; Wu, X.; Shen, J. Extended state observer based fuzzy model predictive control for ultra-supercritical boiler-turbine unit. *Appl. Therm. Eng.* **2017**, *118*, 90–100.
8. Ławryńczuk, M. Nonlinear predictive control of a boiler-turbine unit: A state-space approach with successive on-line model linearisation and quadratic optimisation. *ISA Trans.* **2017**, *67*, 476–495.
9. Ionescu, C.M.; Copot, D. Hands-on MPC tuning for industrial applications. *Bull. Pol. Acad. Sci.-Tech. Sci.* **2019**, *67*, 925–945.
10. Maxim, A.; Copot, D.; Copot, C.; Ionescu, C.M. The 5W's for Control as Part of Industry 4.0: Why, What, Where, Who, and When—A PID and MPC Control Perspective. *Inventions* **2019**, *4*, 10.
11. De Keyser, R.; Muresan, C.I.; Ionescu, C.M. An efficient algorithm for low-order direct discrete-time implementation of fractional order transfer functions. *ISA Trans.* **2018**, *74*, 229–238.
12. Sabatier, J.; Agrawal, O.P.; Machado, J.T. *Advances in Fractional Calculus*; Springer: Berlin, Germany, 2007; Volume 4.
13. Podlubny, I. Fractional differential equations. *Math. Sci. Eng.* **1999**, *198*, 244–252.
14. De Keyser, R.; Muresan, C.I.; Ionescu, C.M. Universal direct tuner for loop control in industry. *IEEE Access* **2019**, *7*, 81308–81320.
15. Cajo Diaz, R.A.; Copot, C.; Ionescu, C.M.; De Keyser, R.; Plaza Guingla, D.A. Fractional order PD path-following control of an AR.Drone quadrotor. In Proceedings of the 2018 IEEE 12th International Symposium on Applied Computational Intelligence and Informatics (SACI), Timisoara, Romania, 17–19 May 2018; pp. 291–296.
16. Saleem, A.; Soliman, H.; Al-Ratrout, S.; Mesbah, M. Design of a fractional order PID controller with application to an induction motor drive. *Turk. J. Electr. Eng. Comput. Sci.* **2018**, *26*, 2768–2778.
17. Mohammadikia, R.; Aliasghary, M. A fractional order fuzzy PID for load frequency control of four-area interconnected power system using biogeography-based optimization. *Int. Trans. Electr. Energy Syst.* **2019**, *29*, e2735.
18. Cajo, R.; Muresan, C.I.; Ionescu, C.M.; De Keyser, R.; Plaza, D. Multivariable fractional order PI autotuning method for heterogeneous dynamic systems. *IFAC-PapersOnLine* **2018**, *51*, 865–870.
19. Zeng, G.Q.; Chen, J.; Dai, Y.X.; Li, L.M.; Zheng, C.W.; Chen, M.R. Design of fractional order PID controller for automatic regulator voltage system based on multi-objective extremal optimization. *Neurocomputing* **2015**, *160*, 173–184.
20. Cajo Diaz, R.A.; Mac Thi, T.; Copot, C.; Plaza Guingla, D.A.; De Keyser, R.; Ionescu, C.M. Multiple UAVs formation for emergency equipment and medicines delivery based on optimal fractional order controllers. In Proceedings of the Preprints of the 2019 IEEE International Conference on Systems, Man and Cybernetics (SMC), Bari, Italy, 6–9 October 2019; pp. 328–333.
21. Cajo, R.; Mac, T.T.; Plaza, D.; Copot, C.; De Keyser, R.; Ionescu, C. A survey on fractional order control techniques for unmanned aerial and ground vehicles. *IEEE Access* **2019**, *7*, 66864–66878.
22. Muresan, C.; Birs, I.R.; Folea, S.; Ionescu, C.M. Fractional order based velocity control system for a nanorobot in non-Newtonian fluids. *Bull. Pol. Acad. Sci.-Tech. Sci.* **2018**, *66*, doi:10.24425/bpas.2018.125946.
23. Zhang, R.; Zou, Q.; Cao, Z.; Gao, F. Design of fractional order modeling based extended non-minimal state space MPC for temperature in an industrial electric heating furnace. *J. Process Control* **2017**, *56*, 13–22.
24. Chen, M.R.; Zeng, G.Q.; Dai, Y.X.; Lu, K.D.; Bi, D.Q. Fractional-Order model predictive frequency control of an islanded microgrid. *Energies* **2019**, *12*, 84.
25. Zhao, S.; Maxim, A.; Liu, S.; De Keyser, R.; Ionescu, C. Effect of control horizon in model predictive control for steam/water loop in large-scale ships. *Processes* **2018**, *6*, 265.

26. De Keyser, R. Model based predictive control for linear systems. In *UNESCO Encyclopaedia of Life Support Systems, Robotics and Automation, Vol XI, Article Contribution 6.43.16.1*; Eolss Publishers Co Ltd.: Oxford, UK, 2003.
27. Romero, M.; de Madrid, A.P.; Vinagre, B.M. Arbitrary real-order cost functions for signals and systems. *Signal Process.* **2011**, *91*, 372–378.



© 2020 by the authors. Licensee MDPI, Basel, Switzerland. This article is an open access article distributed under the terms and conditions of the Creative Commons Attribution (CC BY) license (<http://creativecommons.org/licenses/by/4.0/>).